Acoustic detection of high-energy electrons in a superconducting niobium resonant bar

2006 Europhys. Lett. 76 987

(http://iopscience.iop.org/0295-5075/76/6/987)

EUROPHYSICS LETTERS 15 December 2006

Europhys. Lett., **76** (6), pp. 987–993 (2006)
DOI: 10.1209/epl/i2006-10400-6

Acoustic detection of high-energy electrons in a superconducting niobium resonant bar

M. Bassan[1,2], D. Blair[3], B. Buonomo[4], G. Cavallari[4,5], E. Coccia[1,2], S. D' Antonio[1,2], G. Delle Monache[4], D. Di Gioacchino[4], V. Fafone[1,4], C. Ligi[4], A. Marini[4](*), G. Mazzitelli[4], G. Modestino[4], G. Pizzella[1,4], L. Quintieri[4], S. Roccella[4](**), A. Rocchi[1,2], F. Ronga[4], P. Tripodi[4] and P. Valente[4](***)

[1] *Dipartimento di Fisica, Università Tor Vergata - I-00133 Roma, Italy*
[2] *INFN, Sezione Roma2 - I-00133 Roma, Italy*
[3] *Department of Physics, University of Western Australia Nedlands, WA 6907, Australia*
[4] *INFN, Laboratori Nazionali di Frascati - I-00044 Frascati, Italy*
[5] *CERN - Geneva 23, Switzerland*

received 29 August 2006; accepted in final form 27 October 2006
published online 23 November 2006

PACS. 04.80.Nn – Gravitational wave detectors and experiments.
PACS. 61.82.-d – Radiation effects on specific materials.
PACS. 74.25.-q – Properties of type I and type II superconductors.

Abstract. – We have performed an experiment based on a suspended cylindrical bar, hit by an electron beam, for investigating the results on cosmic rays detected by the gravitational wave antenna Nautilus. The experiment is aimed at measuring the amplitude of the fundamental longitudinal mode of oscillation of a niobium bar, excited by the pressure impulse due to the local interactions of high-energy electrons. We report on the amplitude measurements in a wide temperature range. For niobium in normal state the amplitude agrees within few percents with the predictions of the underlying theory. The amplitude shows a discontinuity at the temperature of transition to superconducting state and, in this state, we measure a reduced amplitude with respect to the normal state. Data in the superconducting state are compared with two models.

Introduction. – The gravitational wave antenna Nautilus, a massive (2.3 tonne) resonant cylindrical bar made of an aluminum alloy (Al5056; Al content ∼95%), has detected very high-energy cosmic rays at a rate higher than expected when the bar was operated at $T = 0.14\,\mathrm{K}$, that is in the superconducting state [1, 2]. On the contrary, the observed rate of high-energy cosmic rays was in agreement with expectations when the bar was operated at $T = 1.5\,\mathrm{K}$, that is in the normal state [3]. The expectations relied on the thermo-acoustic model (TAM), which accounts for the excitations of the longitudinal modes of vibration of a cylinder due to

(*) E-mail: alessandro.marini@lnf.infn.it
(**) Also at Dipartimento di Ingegneria Strutturale e Geotecnica, Università La Sapienza - Roma, I-00184 Italy.
(***) Now at INFN, Sezione Roma1 - I-00185 Roma, Italy.

the energy lost by particles in the interaction, inducing a local heating of the material with a consequent thermal expansion [4–12]. According to TAM applied to a thin cylinder, if a particle normally impinges on the center of the generatrix then the maximum amplitude of the first longitudinal mode of oscillation (FLMO) is given by [6]

$$B_0 = \frac{2\alpha LW}{\pi c_V M} , \tag{1}$$

where L and M are length and mass of the cylinder, W is the total energy lost by the particle in the cylinder, α and c_V are the linear thermal expansion coefficient and the isochoric specific heat of the material, respectively. Moreover, the ratio α/c_V contributes to the definition of the material Grüneisen parameter $\gamma = \beta K_T/\rho c_V$, where β is the volume thermal expansion coefficient ($\beta = 3\alpha$ for cubic solids), K_T is the isothermal bulk modulus and ρ is the density. A possible explanation of the Nautilus results on cosmic-ray detection is related to the antenna conducting state. In order to investigate this possibility we are performing an experiment based on suspended small cylindrical bars, operated both in normal (n) and in superconducting (s) state, exposed to an electron beam of known energy and particle content. A first result of the experiment was the TAM assessment for an Al5056 bar in the temperature range 4.5–270 K, showing an agreement within 10% with predictions [13].

In order to experimentally study the behavior of a resonant detector in the s state, we used a niobium bar, which is in the s state at temperatures below 9 K.

Experimental setup and procedures. – Details on the experiment setup, calibration procedure and simulations can be found in [13]. In brief, the Frascati Linac Beam Test Facility [14] delivers to the bar single pulses of ~ 10 ns duration, containing N_e electrons of 510 ± 2 MeV energy. N_e ranges from about 5×10^7 to 10^9 and is measured with an accuracy of $\sim 3\%$ (for $N_e > 5 \times 10^8$) by an integrating current transformer placed close to the beam exit point. The test mass is a cylindrical bar (0.05 m radius (R), 0.274 m length, 18.43 kg mass) made of Nb (purity $> 99\%$). The bar is hanged inside the cryostat by a multi-stage suspension system insuring an attenuation on the external mechanical noise of -150 dB in the 1700–6500 Hz frequency window. Two piezoelectric ceramics (Pz), electrically connected in parallel, are glued in the position opposite to the bar suspension point and are squeezed when the bar shrinks. In this configuration the strain measured at the bar center is proportional to the displacement of the bar end faces. The Pz output is first amplified and then sampled at 100 kHz by an ADC embedded in a VME system. The measurement of the Pz conversion factor λ, relating voltage to oscillation amplitude, is done according to a procedure [15] based on the injection in the Pz of a sinusoidal waveform of known amplitude, with FLMO frequency f_0 and with time duration less than the decay time of the FLMO mechanical excitations. The procedure is correct if $R/L \ll 1$ and a 6% systematic error in the determination of λ was found for the Nb and Al5056 bars ($R/L \sim 0.18$) [13]. The frequency f_0 increases from 6377.50 to 6569.38 Hz and the factor λ decreases from 1.80×10^7 to 1.50×10^7 V/m in the temperature interval ranging from 270.0 down to 4.5 K. The FLMO maximum amplitude X_{meas} is measured according to $X_{meas} = V_{0,meas}/(G\lambda)$, where G is the amplifier gain and $V_{0,meas}$ is the maximum of the signal component at frequency f_0, which is obtained by Fast Fourier Transform algorithms applied to the digitized Pz signals. A systematic error of $\sim 7\%$, obtained by combining beam monitor and λ determination accuracies, affects X_{meas}.

Data collection and comparison with expectations. – For the n state X_{meas} is compared to the expected value from TAM:

$$X_{therm} = B_0(1 + \epsilon) , \tag{2}$$

Table I – *Thermophysical parameters* (α, c_V) *and expected normalized FLMO maximum amplitude* (X_{therm}/W) *as a function of temperature* (T)*. TAM assessment: fit coefficient* (m) *and error* (Δm)*.*

T (K)	α [Ref.] ($10^{-7}\,\mathrm{K}^{-1}$)	c_V [Ref.] ($\mathrm{J\,mol}^{-1}\,\mathrm{K}^{-1}$)	X_{therm}/W ($10^{-10}\,\mathrm{m\,J}^{-1}$)	m	Δm
275.0	69.8 [16]	24.5 [17]	2.31	0.96	0.01
81.0	41.9 [16]	14.7 [17]	2.30	1.03	0.01
12.5	0.69 [18]	0.36 [19]	1.55	0.95	0.02

where the subscript *therm* stands for thermal effects and ϵ is a corrective parameter estimated by a Monte Carlo (MC) simulation [13], which takes into account the solutions $\mathrm{O}[(R/L)^2]$ for the modes of oscillation of a cylinder, the transverse dimension of the beam at the impact point (diameter $\sim 2\,\mathrm{cm}$) and the trajectories of the secondary particles generated in the bar. The MC estimated value of ϵ is -0.08 for the Nb bar. MC simulation of 10^6 electrons of 510 MeV energy interacting with the bar also predicts an average energy loss $\Delta E \pm \sigma_{\Delta E} = 453 \pm 39\,\mathrm{MeV}$ per electron, leading to a total energy loss estimate $W = N_e \times \Delta E$ per beam pulse. In order to compute X_{therm} for each beam pulse, interpolations of thermophysical data in the literature give the values of α and c_V at different temperatures, when parameterizations are not readily available (table I). At fixed temperature the comparison between measured and expected values of X is given by the parameter m fitting the relation $X_{meas} = mX_{therm}$. Figure 1 shows the comparisons at $T = 12.5, 81.0, 275.0\,\mathrm{K}$ and table I summarizes the values of m and the error Δm obtained by the fit procedure. This error is in agreement with the one expected from the fluctuations in the measurement of the FLMO amplitude and of the beam pulse charge. The values obtained for m suggest a good agreement in a wide range of temperature between the TAM predictions for X and the measurements, when experimental uncertainties are taken into account.

Then we measured the amplitude of the oscillations induced by the beam pulses when the bar was in the s state. The linear dependence of X_{meas} on the measured energy deposited by the beam pulses in the bar at $T = 4.5\,\mathrm{K}$ is shown in fig. 2. The onset of effects related to the s state at the critical temperature $T_c \sim 9\,\mathrm{K}$ and the behavior of X_{meas}/W above and below T_c are shown in fig. 3. Bands in fig. 3 represent the expected values of $(X_{therm} \pm \Delta X_{therm})/W$, computed with thermophysical parameters for the n state $(T > T_c)$ and s state $(T < T_c)$. The evaluation of X_{therm} for the s state is made by taking into account

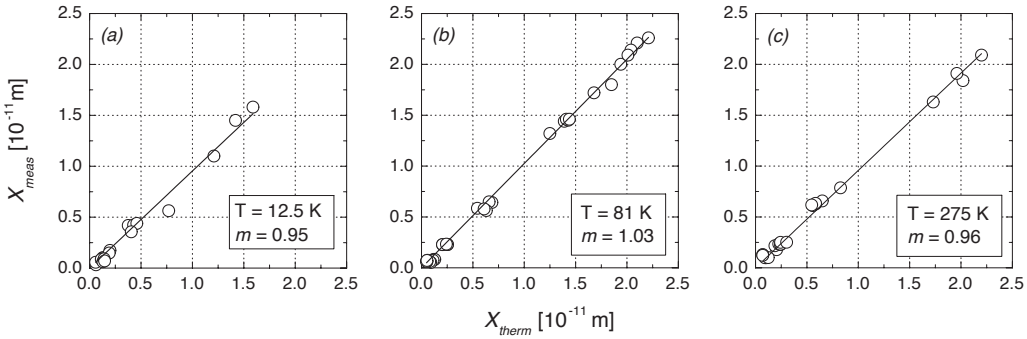

Fig. 1 – $T = 12.5\,\mathrm{K}$ (a), 81 K (b), 275 K (c). Measured FLMO maximum amplitudes (X_{meas}) for different N_e are plotted *vs.* expected values (X_{therm}). The insets show the results of the fit $X_{meas} = mX_{therm}$.

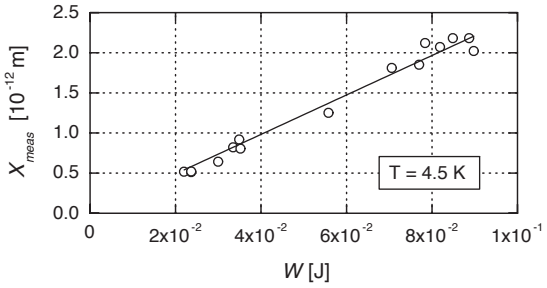

Fig. 2 – $T = 4.5\,\mathrm{K}$. Correlation between measured FLMO maximum amplitudes (X_{meas}) and energy (W), deposited by beam pulses in the bar, as derived by N_e measurements.

that $\alpha^s = \alpha_l^s + \alpha_e^s$, where for the lattice contribution $\alpha_l^s(T) = \alpha_l^n(T)$ is assumed, and α_e^s is the electronic contribution. Interpolations on data of refs. [20] and [21] give $\alpha_e^s(T)$ and $c_V^s(T)$ respectively, the parametrization in [18] is used for computing $\alpha_l(T)$ and ΔX_{therm} is evaluated by combining the quoted uncertainties on α and c_V. Table II shows the thermophysical parameters obtained by this procedure for selected temperatures. Measured values of X/W at $T < T_c$ show a qualitative agreement with expectations based only on thermal effects evaluated with thermophysical data for the s state.

An alternate approach for interpreting the measurements at $T < T_c$ takes into account local transitions in zones centered around the particle paths [7, 9]. Two acoustic sources are related to a particle impinging on a bar made of a material in the s state. The first source is due to s-n local transitions caused by the interaction of the particle with the material in the s state and the second is related to thermal effects in the n state, as described by relation (2). As a consequence, the FLMO amplitude X has two components: X_{tr} and X_{therm}, the first due to s-n transitions and the latter related to thermal effects. In order to verify this hypothesis,

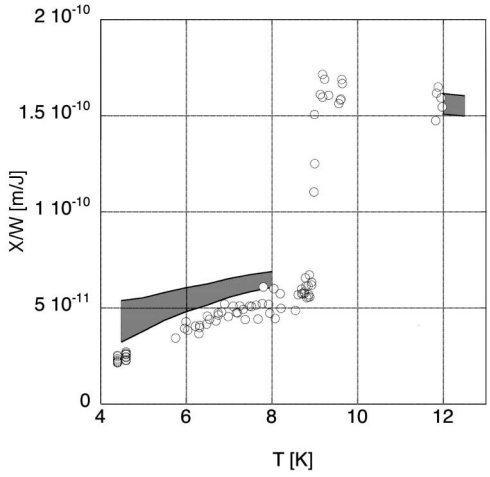

Fig. 3 – FLMO maximum amplitudes (X) normalized to the total energy lost per beam pulse (W) *vs.* temperature (T). Circles: measured values. Bands: expected values of X_{therm}/W from thermophysical data for pure Nb in the n state ($T \sim 12\,\mathrm{K}$) and in the s state ($T < 9\,\mathrm{K}$).

Table II – *Thermophysical parameters* (α, c_V) *for pure* Nb *in the* n *and* s *state.*

T (K)	α^n [18] ($10^{-8}\,\mathrm{K}^{-1}$)	c_V^n [21] ($\mathrm{J\,mol}^{-1}\,\mathrm{K}^{-1}$)	α^s [18,20] ($10^{-8}\,\mathrm{K}^{-1}$)	c_V^s [21] ($\mathrm{J\,mol}^{-1}\,\mathrm{K}^{-1}$)
8.0	2.8	0.13	1.7	0.22
6.0	1.8	0.07	0.6	0.09
4.5	1.2	0.05	0.2	0.04

we plot in fig. 4 the observed values of X_{tr}/W, obtained by subtracting the expected values due to thermal effects in the n state from the measured values of X/W:

$$\left(\frac{X_{tr}}{W}\right)_{obs} = \frac{X_{meas} - X_{therm}}{W}.$$

Only measured values related to beam pulses with electron content $N_e > 10^9$ are displayed in the plot in order to minimize the fluctuations in the N_e measurement. In evaluating X_{therm} we use the parametrization given in ref. [18] for $\alpha^n(T)$ and interpolations of data in ref. [21] for $c_V^n(T)$ (see table II). Errors on $(X_{tr}/W)_{obs}$, estimated by combining the measurement errors and the quoted uncertainties on the thermophysical parameters, are of the order of 6-7%.

In order to compare the observed values of X/W with the expected ones, we note that the ratio of the two components is [7]

$$\frac{X_{tr}}{X_{therm}} = \frac{K_T A \Delta V/V}{\gamma \mathrm{d}E/\mathrm{d}x}, \tag{3}$$

where A is the cross-section of the zone switched from s to n state, $\Delta V/V$ is the specific difference of volumes between s and n states, γ is the Grüneisen parameter for the n state and $\mathrm{d}E/\mathrm{d}x$ is the specific energy loss of the particle in the material. The cross-section A is given by the relation [22] $A = (\mathrm{d}E/\mathrm{d}x)/(\Delta\mathcal{H}/V)$, which involves the specific difference of enthalpies,

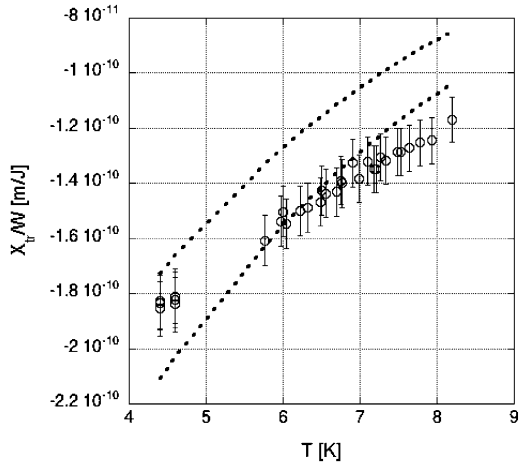

Fig. 4 – The component of the FLMO maximum amplitude due to local transitions normalized to the energy lost (X_{tr}/W) *vs.* temperature (T). Circles : observed values with errors. The region enclosed by the broken lines shows the expected values, computed assuming an error of 10% on $(\partial H_c/\partial P)$.

$\mathcal{H}$, among the two states. By introducing the thermodynamic critical field H_c [23], which can be defined for a type-II superconductor, the following relations hold at the first order [24]: $\Delta V/V = (V_n - V_s)/V = H_c(\partial H_c/\partial P)/(4\pi)$, $\Delta\mathcal{G}/V = (\mathcal{G}_n - \mathcal{G}_s)/V = H_c^2/(8\pi)$ and $\Delta\mathcal{S}/V = (\mathcal{S}_n - \mathcal{S}_s)/V = -H_c(\partial H_c/\partial T)/(4\pi)$, where $\mathcal{G}$ is the Gibbs free energy, $\mathcal{S}$ is the entropy and P is the pressure. A H_c-dependance from the reduced temperature $t = T/T_c$, given by $H_c(t) = H_c(0)(1-t^2)$, is assumed and BCS theory of superconductivity predicts $H_c(0) \sim 2.43\Gamma^{1/2}T_c$, with Γ the electronic specific-heat coefficient per unit volume for the n state. The following values are available for pure Nb: $\Gamma = 6.88 \times 10^3\,\mathrm{erg\,cm^{-3}\,K^{-2}}$ for $T > 3\,\mathrm{K}$ [25], which gives $H_c(0) = 1814\,\mathrm{Oe}$, and $(\partial H_c/\partial P)_0 = (-1.2 \pm 0.1) \times 10^{-9}\,\mathrm{Oe\,dyn^{-1}\,cm^2}$ [16]. The use of the above indicated thermodynamic relations involving $\mathcal{G}$ and $\mathcal{S}$ together with $\Delta\mathcal{H} = \Delta\mathcal{G} + T\Delta\mathcal{S}$ allows to obtain $\Delta\mathcal{H}/V = H_c^2(0)(1-t^2)(1+3t^2)/(8\pi)$. We now combine relations (1), (2), (3) and the definition of γ to derive the expected values of X_{tr}/W as a function of T:

$$\left(\frac{X_{tr}}{W}\right)_{exp} = \left\{\frac{X_{therm}}{W}\right\}\left\{\frac{X_{tr}}{X_{therm}}\right\} = \frac{2L(1+\epsilon)\rho(\Delta V/V)}{3\pi M(\Delta\mathcal{H}/V)}.$$

These expected values, which have at least a 10% uncertainty due to the error on $(\partial H_c/\partial P)$, are displayed in fig. 4 as the region enclosed by the broken lines. Figure 4 shows that the observed values of X_{tr}/W fairly agree with the expected ones within the uncertainties.

Conclusions. – In summary, we report on measurements of mechanical oscillations of a suspended resonant Nb bar due to the energy lost by high-energy electrons interacting in the bulk. In the temperature range 4.5–275 K the maximum amplitude of the fundamental longitudinal mode is found to be proportional to the total energy deposited by the electron beam. For temperatures greater than T_c the amplitude measurements agree within the experimental uncertainties with the thermal effects, predicted by TAM and based on the ratio α/c_V. Measured values of the amplitudes show a discontinuity across T_c. For the s state, although the amplitudes are quite consistent with a model based on thermal effects only, a possible better agreement is found with models which include: a component related to local transitions in small zones centered on the paths of the high-energy particles interacting in the bulk and a component related to thermal effects for the n state. Charged cosmic rays impinging on gravitational wave resonant detectors or on the mirrors of interferometric detectors could be an important source of noise for future experiments. The change of the oscillation amplitude, related to the state of conduction of a gravitational wave resonant detector, was not taken into account in the past, when effects of cosmic rays in the bar were evaluated using TAM. Here we have experimentally shown that the superconducting state of the bulk should be taken into account in the calculations of the cosmic-ray effects on components of gravitational wave detectors or when small displacements of test masses, which are exposed to high-energy radiation, are relevant.

* * *

This work is partially supported by the EU project ILIAS (RII3-CT-2004-506222).

REFERENCES

[1] Astone P. *et al.*, *Phys. Rev. Lett.*, **84** (2000) 14.
[2] Astone P. *et al.*, *Phys. Lett. B*, **499** (2001) 16.
[3] Astone P. *et al.*, *Phys. Lett. B*, **540** (2002) 179.
[4] Beron B. L. and Hofstadter R., *Phys. Rev. Lett.*, **23** (1969) 184.
[5] Beron B. L. *et al.*, *IEEE Trans. Nucl. Sci.*, **7**, N1 (1970) 65.

[6] Grassi Strini A. M. *et al.*, *J. Appl. Phys.*, **51** (1980) 948.
[7] Allega A. M. and Cabibbo N., *Lett. Nuovo Cimento*, **38** (1983) 263.
[8] Malugin V. A. and Manukin A. B. (1983), as reported in Lyamshev L. M., *Radiation Acoustics* (CRC Press) 2004, p. 301.
[9] Bernard C. *et al.*, *Nucl. Phys. B*, **242** (1984) 93.
[10] De Rujula A. and Glashow S. L., *Nature*, **312** (1984) 734.
[11] Amaldi E. and Pizzella G., *Nuovo Cimento C*, **9** (1986) 612.
[12] Liu G. and Barish B., *Phys. Rev. Lett.*, **61** (1988) 271.
[13] Buonomo B. *et al.*, *Astropart. Phys.*, **24** (2005) 65.
[14] Mazzitelli G. *et al.*, *Nucl. Instrum. Methods A*, **515** (2003) 524.
[15] Pallottino G. V. and Pizzella G., *Nuovo Cimento B*, **45** (1978) 275.
[16] White G. K., *Cryogenics*, **2** (1962) 292.
[17] Gray D. E., Billings B. H., Bleil D. F., Cook R. K., Crosswhite H. M., Frederikse H. P. R., Lindsay R. B., Marion J. B. and Zemansky M. W. (Editors), *American Institute of Physics Handbook*, 3rd edition (McGraw-Hill Book Co.) 1972.
[18] Smith T. F. and Finlayson T. R., *J. Phys. F: Metal Phys.*, **6** (1976) 709; White G. K. *et al.*, *Inst. Phys. Conf. Ser.*, **39** (1978) 420.
[19] Leupold H. A. *et al.*, *J. Low Temp. Phys.*, **28** (1977) 241.
[20] Simpson M. A. and Smith T. F., *J. Low Temp. Phys.*, **32** (1978) 57.
[21] Leupold H. A. and Borse H. A., *Phys. Rev.*, **134** (1964) A1322.
[22] Strehl B. *et al.*, *Phys. Lett. B*, **242** (1990) 285.
[23] We keep the *practical* c.g.s. unit for the magnetic field, as used by the authors of the cited articles, and we convert the density of the magnetic energy to SI units.
[24] Hake R. R., *Phys. Rev.*, **166** (1968) 471.
[25] Moore M. A. and Paul D. I., *Solid State Commun.*, **9** (1971) 1303.